Evaluation of liquid structure for potassium, zinc, and cadmium

S. K. Lai
Department of Physics, National Central University, Chung-li 32054, Taiwan, Republic of China and International Centre for Theoretical Physics, Trieste, Italy

Wang Li
International Centre for Theoretical Physics, Trieste, Italy

M. P. Tosi
Department of Theoretical Physics, University of Trieste, Trieste, Italy and International Centre for Theoretical Physics, Trieste, Italy

(Received 25 June 1990)

The main aim of this work is to give a theoretical interpretation for the "anomalous" liquid-structure factors of zinc and cadmium near freezing and for their variation with temperature, as contrasted with the "normal" behavior of a liquid metal such as potassium. Using an *ab initio* generalized nonlocal model pseudopotential and with two alternative exchange-correlation functions for electronic screening, we construct interionic pair potentials for the above metals. These are then used for liquid-structure calculations within two alternative integral-equation schemes of considerable refinement, namely the modified hypernetted-chain approach of Rosenfeld and Ashcroft [Phys. Rev. A **20**, 1208 (1979)] and the hybridization of the hypernetted chain and the soft-core mean spherical approximations as proposed by Zerah and Hansen [J. Chem. Phys. **84**, 2336 (1986)]. The comparison between the theoretical results for the temperature dependence of the liquid-structure factor of potassium and very recent neutron-diffraction data gives us confidence in the high reliability of the pseudopotential in the present integral-equation schemes. The same approach is then extended to investigate the liquid-structure factors for zinc and cadmium near their freezing temperature and at a few temperatures above freezing. We find that the asymmetric shape of the main peak in the structure factor of these elements near freezing can be understood in terms of the role of the medium- and long-range interaction parts in the pair potential. Our results also shed some light on the subtle changes of the liquid structure of these divalent metals with temperature, and specifically on the thermal influence in restoring the skewed shape of the main peak back to a normal symmetric shape at much higher temperatures.

I. INTRODUCTION

Central to an understanding of the electronic and thermodynamic properties for simple liquid metals is the liquid-structure factor [hereafter referred to as $S(q)$] describing the ion-ion correlations in equilibrium. This quantity can be evaluated by several different routes, given an accurate knowledge of the effective interatomic forces. The most direct means is by computer simulation. This approach generally produces a remarkably accurate pair-correlation function for efficient algorithms, such as the numerical integration code[1] in the case of molecular dynamics or the Markov chain stochastic technique[2] in the case of Monte Carlo simulation. There are, however, notable inadequacies in using simulation data to extract $S(q)$. The pair-correlation function [to be denoted by $g(r)$] is known only over a limited range of interionic distance, and hence the problem of Fourier transformation leading to $S(q)$ entails uncertainties in the low momentum-transfer region. Computer simulation is also less informative in the small-r region of $g(r)$, which is most interesting in relation to the statistical-mechanical theory of fluids.[3]

As an alternative to computer simulation, one may attempt to calculate $S(q)$ and $g(r)$ by using variants of the statistical-thermodynamical theory of fluids.[4,5] A well-known approach is based on thermodynamic-perturbative theories. In such theories, the basic step consists of finding a reference system which is adapted to construct the Helmholtz free energy of the liquid metal in terms of suitable expansion parameters. The variational theory based on the Gibbs-Bogoliubov inequality[6,7] represents such a technique, which is devised to model the structure factor $S(q)$ of a liquid metal by an appropriate reference $S_{\rm ref}(q;\nu,\dots)$, $\nu,\dots$ being parameters characterizing the reference fluid. According to the inequality the liquid-metal Helmholtz free energy is a bounded function consisting of the reference free energy plus the expansion parameter which, in this case, is the difference in potential energies between the real and the reference fluid, calculated with $S_{\rm ref}(q;\nu,\cdots)$. Evaluation of $S_{\rm ref}(q;\nu,\cdots)$ is accomplished by searching for the extremum of the free energy.

Another widely used thermodynamic perturbation theory is the Weeks-Chandler-Andersen[8] (WCA) scheme. In this approach one starts with an interionic potential

$V(r)$, which is first separated into a repulsive part $\varphi_r(r)$ and a long-range attractive part $\varphi_l(r)$. By invoking the ansatz that the density correlations in a highly dense fluid are dominated by the excluded volume effect, it can be shown[9] that the WCA Helmholtz free energy of a liquid metal has an identical form to that of the variational theory. However, the physical content and the detailed means to obtain $S(q)$ in the Gibbs-Bogoliubov inequality approach and in the WCA perturbation theory are somewhat different. Whereas in the former $S_{\rm ref}(q;\nu,\dots)$ is modeled *variationally* via a chosen fluid system (such as the neutral hard-sphere system or the one-component plasma), the corresponding structure factor in the latter is determined *perturbatively* by the short-range repulsion $\varphi_r(r)$ which, in turn, is customarily expanded with respect to a neutral hard-sphere system. Several authors[10-15] have applied this approach to the study of liquid structure for a number of simple metals. Invariably, it is found that, although the characteristic softness of a liquid-metal potential can be accounted for, the calculated medium-range structure is still inaccurate, being affected by a shift in phase of oscillations. These studies have shown that the above approaches, apart from the ease of simultaneously yielding the values of thermodynamic functions, can only describe $S(q)$ semiquantitatively.

Further progress in the calculation of $S(q)$ has emerged from two closely similar approaches, which may be called the WCA and the one-component-plasma (OCP) random-phase approximation (RPA). In both these theories, the contribution of the long-range attraction $\varphi_l(q)$ to $S(q)$ is accounted for within the RPA for the Ornstein-Zernike direct-correlation function of the liquid. The main difference in the WCA RPA and OCP RPA lies in the treatment of the unperturbed reference system. In the WCA-RPA method one treats the unperturbed reference part by a method similar to that described above for the WCA thermodynamic perturbation theory, whereas in the OCP-RPA method the unperturbed reference potential is modeled by the direct Coulomb interaction of the "bare" ions and $\varphi_l(r)$ is thus related entirely to the indirect ion-ion screening term. Both the WCA-RPA (Ref. 16) and the OCP-RPA (Refs. 17-20) approaches have been applied with varying degrees of success to the study of $S(q)$ for all liquid alkali metals[21] and several polyvalent metals. The applicability of both these theories is limited, however, to the low-angle scattering region and to thermodynamic states that are not too far from the freezing point.

A number of authors have attempted to circumvent this inherent weakness of the RPA method. The central idea underlying the so-called optimized RPA (Ref. 22) is to give attention to the behavior of the attractive term in the excluded volume region, with the aim of preserving the property that the pair-correlation function should remain essentially zero inside a region of space in which penetration is prohibited by the interparticle repulsions. Depending on the liquid metal of interest, both the WCA (Refs. 12-14, 23, and 24) and OCP (Ref. 25) versions of the optimized RPA have been developed. Here it suffices to stress two points. First, the above-mentioned works[12-14,23-25] have shown that, quite generally, the optimized RPA yields marked improvement over the RPA scheme in the liquid alkali metals and a few polyvalent metals. Second, the usefulness of the method appears to be somewhat dependent on the choice of the reference system used. Indeed, on the one hand, Pastore and Tosi[25] applied successfully the optimized OCP RPA and obtained very good agreement with simulation data and experiment for liquid Rb and other alkali metals near freezing, while, on the other hand, Kahl and Hafner,[12] using the optimized WCA RPA, were unable to obtain the optimal potential for Rb in the same thermodynamic state.[26] Obviously there still is a need for more work to assess the potentiality of this approach.

There is yet another avenue to a theoretical study of $S(q)$, which is the thermodynamically self-consistent integral-equation method which has received revived interest in the past few years. There are at least two reasons for this. From the practical viewpoint, while in the traditional integral-equations method, given a closure for the Ornstein-Zernike equation, the iterative procedure to obtain a solution for the pair-correlation function often proceeds inefficiently,[5] elegant algorithms[27] have become available for carrying out such a procedure efficiently. This technical advance has stimulated the study of more refined methods for obtaining $S(q)$, since, as mentioned just above, even the best thermodynamic perturbation approach is only partially successful in its predictions for $S(q)$. In this work we adopt (i) the self-consistent modified hypernetted chain[3,28] (MHNC) and (ii) the "mixture" of HNC and soft-core mean spherical approximation[29] (HMSA) integral-equation techniques for an investigation of the liquid structure of Zn and Cd. We are motivated partly by the recent work of Pastore and Kahl,[30,31] who applied these techniques successfully to liquid alkali metals, and partly by the fact that these elements are intrinsically interesting by having "anomalous" liquid-structure factors. Specifically, their structure factors show asymmetric shapes in the main peak at or near the melting point, which are seen to disappear gradually as temperature increases. To our knowledge, such a behavior of $S(q)$ has not been studied beyond a speculative discussion by Weaire[32] and the optimized RPA calculations by Regnaut, Badiali, and Dupont[23] and by Hafner and Kahl.[24] In order to investigate quantitatively the factors that contribute to this behavior, we have combined the above-mentioned integral-equation theories with a highly reliable generalized nonlocal model pseudopotential of Li, Li, and Wang[33] which we first examine for liquid K as a means to ascertain its reliability as applied to a normally symmetric $S(q)$. In connection with our choice of integral-equation methods, it is perhaps relevant to note that the MHNC integral-equation theory has already been applied successfully to the study of the OCP system both for bulk[34] and surface[35] properties. Very recently, it has also been applied by Hoshino *et al.*[36] to explain the temperature dependences of the $S(q)$ of expanded liquid Cs. Much less work has been devoted to the HMSA method,[37,38] however.

The layout of the paper is as follows. In Sec. II we summarize the essential ingredients needed in the present

study and give some computational details. Section III presents our numerical results. Here we compare the results first for liquid K with very recent experiments[39,40] at various temperatures and then for liquid Zn and Cd metals at those temperatures at which experiments are available.[41–45] We discuss quantitatively also the factors that give rise to such anomalous behavior of the structure factor. Finally in Sec. IV we give our summary and concluding remarks.

II. INTEGRAL-EQUATION METHOD

In this section we summarize in Secs. II A and II B the three basic ingredients—the interatomic pair potential, the HMSA and MHNC theories, and the choice of bridge functions in the latter—to be used in our integral-equation calculations.

A. Interatomic pair potential

Given a system of N pseudoatoms confined in a volume Ω at a given density $\rho=N/\Omega$ and temperature T, we assume that they interact via a symmetric pairwise potential $V(r)$ which is constructed using the modified generalized nonlocal model pseudopotential (GNMP) of Li, Li, and Wang.[33] Following Li, Li, and Wang and Wang and Lai[46] we may write

$$V(r)=\frac{Z_{\rm eff}^2}{r}\left[1-\frac{2}{\pi}\int_0^\infty dq\, G_N(q)\frac{\sin qr}{q}\right], \tag{1}$$

where $G_N(q)$ is the normalized energy-wave-number characteristics and $Z_{\rm eff}^2=Z^2-\rho_d^2$, Z and ρ_d being the nominal valence and the depletion charge, respectively. It is worthwhile to emphasize that in the work of the above authors proper attention has been given to the one-electron energy and pseudo-wave-function and that higher-order perturbative corrections have been incorporated through the introduction of a parameter in the bare-ion pseudopotential. The rigorousness of such a procedure has been justified theoretically by Li, Li, and Wang[33] and its reliability is further confirmed by several successful applications to various metallic properties.[47] Consequently we feel that our calculations are based on interionic potentials having a high degree of refinement. We also recall that the calculation of $G_N(q)$ involves a local-field factor for exchange and correlation in electronic screening. We shall present below the results obtained with two alternative choices for this factor.

B. MHNC and HMSA theories

Having described our basic input source $V(r)$, we turn to summarize the essential equations needed in the integral-equation approach. Common to both integral-equation techniques is the Ornstein-Zernike (OZ) equation, given by

$$\gamma(r)\equiv h(r)-c(r)=\rho\int h(r')c(|\mathbf{r}-\mathbf{r}'|)d\mathbf{r}' \tag{2}$$

in which $h(r)=g(r)-1$ and $c(r)$ is the direct correlation function. To solve the OZ integral equation, one needs a closure between $h(r)$ and $c(r)$. A formally exact closure relation is

$$g(r)=\exp[\gamma(r)-\beta V(r)-B(r)], \tag{3}$$

where $B(r)$ is the sum of the "bridge" graphs.[5] [The usual hypernetted-chain approximation corresponds to setting $B(r)=0$.] Given a prescription for $B(r)$, Eqs. (1)–(3) can be solved iteratively to yield $g(r)$.

A number of reliable bridge functions[3,38,48,49] have been proposed in the literature. In the MHNC one takes advantage of the ansatz of universality in the bridge function and adopts the Percus-Yevick (PY) hard-sphere parametrized form of $B(r)$. According to Rosenfeld and Ashcroft,[3] the latter can be written

$$B(r)=\begin{cases}-c_{\rm PY}(r)-1-\ln[-c_{\rm PY}(r)], & r<\sigma\\ g_{\rm PY}(r)-1-\ln g_{\rm PY}(r), & r>\sigma\end{cases}. \tag{4}$$

The advantage of using Eq. (4) is that $B(r)$ is a function of a single parameter $\eta=\pi\rho\sigma^3/6$ and that analytical expressions for $g_{\rm PY}(r)$ and $c_{\rm PY}(r)$ are available.[50,51]

Coming to the second integral-equation approach, we note that the HMSA is essentially a generalization of the thermodynamical self-consistent closure of Rogers and Young,[38] interpolating continuously between the soft-core mean spherical approximation (MSA) equation[52] at small r and the HNC closure at large r. Implementation of this integral-equation scheme is slightly more involved. First, $V(r)$ is split into $\varphi_r(r)$ and $\varphi_l(r)$, the short-range and long-range terms respectively, according to

$$\varphi_r(r)=\begin{cases}V(r)-V(r_m), & r\le r_m\\ 0, & r\ge r_m\end{cases}$$
$$\varphi_l(r)=\begin{cases}V(r_m), & r\le r_m\\ V(r), & r\ge r_m\end{cases}, \tag{5}$$

where $V(r_m)$ is the pair potential evaluated at its first-minimum position r_m. Next, by virtue of Eq. (5) Zerah and Hansen[29] proposed

$$g(r)=\exp[-\beta\varphi_r(r)]\left[1+\frac{\exp\{f(r)[\gamma(r)-\beta\varphi_l(r)]\}-1}{f(r)}\right] \tag{6}$$

in which

$$f(r)=1-\exp(-\alpha r), \tag{7}$$

where α is a mixing parameter to be discussed immediately below. As can be seen, the "switching function" $f(r)$ satisfies, on the one hand, the limiting behavior

$$\lim_{r\to 0} f(r)=0 \tag{8}$$

[so that Eq. (6) reduces in this limit to the soft-core MSA closure] and, on the other hand, the limiting behavior

$$\lim_{r\to\infty} f(r)=1, \tag{9}$$

corresponding to the HNC closure.

We turn next to discuss the determination of the packing fraction η in the MHNC and the parameter α in the HMSA. Following a customary procedure, we relate the determination of these adjustable parameters to consistency between the isothermal compressibility obtained from the long-wavelength limit of $S(q)$,

$$\chi_T=\beta\rho^{-1}\left[1+4\pi\rho\int[g(r)-1]r^2dr\right], \tag{10}$$

and that obtained by an alternative route. The virial route is often chosen, leading for a metal to the expression

$$\begin{aligned}(\chi_T^V)^{-1}=\rho\beta^{-1}+\rho&\left[2n\frac{du(n)}{dn}+n^2\frac{d^2u(n)}{dn^2}\right]\\&+2\pi\rho^2\int_0^\infty dr\,r^2\left[\frac{r}{3}\frac{\partial}{\partial r}-n\frac{\partial}{\partial n}\right]g(r)\\&\times\left[\frac{r}{3}\frac{\partial}{\partial r}-n\frac{\partial}{\partial n}\right]V(r)\\&+2\pi\rho^2\int_0^\infty dr\,r^2g(r)\left[\frac{r}{3}\frac{\partial}{\partial r}-n\frac{\partial}{\partial n}\right]^2V(r),\end{aligned} \tag{11}$$

where the superscript V denotes the virial pressure route. In the above, n is the electronic density and $u(n)$ is the structure-independent contribution to the energy, consisting of the ground-state electron-gas energy, the average interaction between electrons and the non-Coulombic part of the bare-ion pseudopotential (first-order pseudopotential) and other self-energy terms (for the GNMP theory, see Lai[47]). Equation (11) follows by the well-known homogeneous deformation method of calculating the isothermal compressibility and has been widely used in the literature.[53–55]

The evaluation of Eq. (11) can be quite delicate, in view of the comparatively less accurate $u(n)$ term.[53,55–57] In this work, instead of using the full form of Eq. (11), we adopt a different self-consistency condition. To this end, we note two relevant points. First, as an alternative to Eq. (10) which determines χ_T from $S(0)$ through a calculation with interionic interactions at constant volume, there is a computationally convenient way of calculating the isothermal compressibility of a metal by the so-called method of long waves (LW).[53,55,58,59] In this method one sets out to consider a total-energy expression of the form

$$\Phi(\{N\})=Nu(n_0)+\tfrac{1}{2}\sum_{\substack{i,j\\i<j}}V(r;n_0)+\cdots, \tag{12}$$

where N is the total number of ions and the electron density n_0 is kept fixed at the appropriate thermodynamic state throughout. The expression for χ_T that follows from Eq. (12) (see Ref. 59) can be shown to be equivalent to that in Eq. (10).[53] Second, it has been pointed out[54,55,58,59] that the χ_T obtained by the LW method and that obtained by the homogeneous deformation route are in principle equivalent, provided one carries out the perturbation calculation to an infinite order. Nevertheless, within second-order perturbation theory, it was also found[53,55,58,59] that the homogeneous deformation route invariably yields a χ_T value which differs from that in the LW approach using Eq. (12).

With these two points in mind, and aiming only at statistical-mechanical self-consistency for liquid structure at fixed density, we determine the parameter η or α by demanding equality between Eq. (10) and the expression to which Eq. (11) reduces when the density dependences of u and $V(r)$ are dropped. This self-consistency procedure was also followed by Pastore and Kahl[30,31] for alkali metals. We further note that since the GNMP theory adopted here incorporates higher-order corrections to the usual second-order perturbation treatment of the electron-ion interaction, we expect the value of χ_T obtained by this method to be of comparable accuracy as the homogeneous deformation results, thus approximately achieving thermodynamic self-consistency. Indeed, as we shall demonstrate in Sec. III C, in the absence of such higher-order corrections, our integral-equation method produces distinctly poor results for $S(q)$.

III. NUMERICAL RESULTS AND DISCUSSION

In this section we first present our results for liquid K at different temperatures, then the liquid-structure factor of Zn which shows a slight "tilting" behavior, and finally that of Cd having a strongly asymmetric $S(q)$. In all the calculations given below, we adopt two alternative exchange-correlation factors in the pair potential, due to Singwi *et al.*[60] (SI) and to Ichimaru and Utsumi[61] (IU), respectively, and apply them separately in the two integral-equation approximations. For convenience in discussion, we shall adopt the following notation: MHNC-SI means that the integral equation used is the MHNC and the input interionic potential is constructed using the exchange-correlation function of SI. Similar meanings apply to the other symbols.

A. Liquid potassium

As a preliminary test of our integral-equation schemes, we present in Fig. 1 the pair-correlation function for liquid K at freezing calculated in the MHNC and the HMSA, along with the Monte Carlo data of Lai[47] obtained from the same interionic pair potential and SI exchange-correlation factor. The SI $V(r)$ interionic pair potential used in the calculation of $g(r)$ is also given in the same figure, together with the IU $V(r)$ included for comparison. Further details of our results are reported in Table I.

It is immediately evident from Fig. 1 that both the MHNC-SI and the HMSA-SI integral equation produce virtually indistinguishable $g(r)$, which compare rather well with the simulation result particularly in the main maximum and subsequent oscillations. There is a slight overestimation near the second peak of $g(r)$ and this accounts for a small enhancement in oscillation near the second maximum of $S(q)$ relative to experiment[39] (see Fig. 2). We also note that in the low-momentum-transfer region, where electronic screening is most important, our

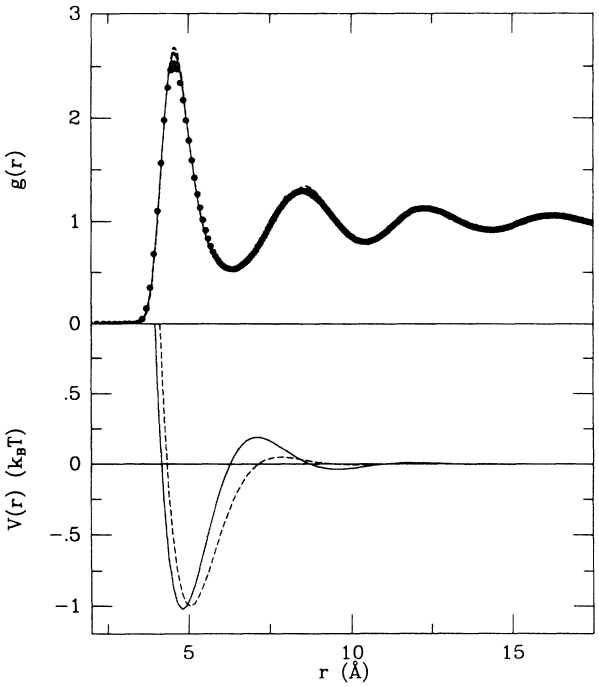

FIG. 1. The pair-correlation function $g(r)$ for liquid K at freezing calculated in the MHNC-SI (full curve) and HMSA-SI (dashed curve) compared with the Monte Carlo data (solid circles) of Lai (Ref. 47). For the interionic pair potentials, we include the IU $V(r)$ (full curve) and SI $V(r)$ (dashed curve) for comparison.

calculated $S(q)$ ($0 \leq q \leq 1$ Å^{-1}) agrees with experiment within about 10%, as indicated in the magnified insert in Fig. 2. The above calculations have been repeated at $T=338$ K by replacing the SI local-field corrections function with the IU one. Except for a minor but noticeable improvement shown by the HMSA-IU structure factor in the proximity of the second peak, both the MHNC-IU and HMSA-IU structure factors do not differ visibly from those given in Fig. 2 and accordingly we do not present them here. Thus, the overall quality of our theoretical $S(q)$ can be considered to be very satisfactory for *all* wave vectors.

To make a further check on our present approach, we extend our calculations on liquid K to several elevated temperatures ($T=373$, 573, 773, and 973 K) for which very recent neutron diffraction data[39,40] are available. Our MHNC-SI results for $S(q)$ at different temperatures are depicted in Fig. 3 together with the experimental data of van der Lugt and Alblas[39] at $T=373$ K and of Jal, Mathieu, and Dupuy[40] for all the other temperatures. It is gratifying to see that our theoretical results compare very closely with these observations not only near freezing but also at temperatures up to 973 K. These results are of a much better quality than those calculated using (i) the Gibbs-Bogoliubov inequality (compare, for example, Akinlade, Lai, and Tosi[62]) and (ii) a similar MHNC approach of Kahl and Pastore[31] involving a local empty-core pseudopotential. Again upon repeating the calculations with the HMSA-SI at all temperatures of interest

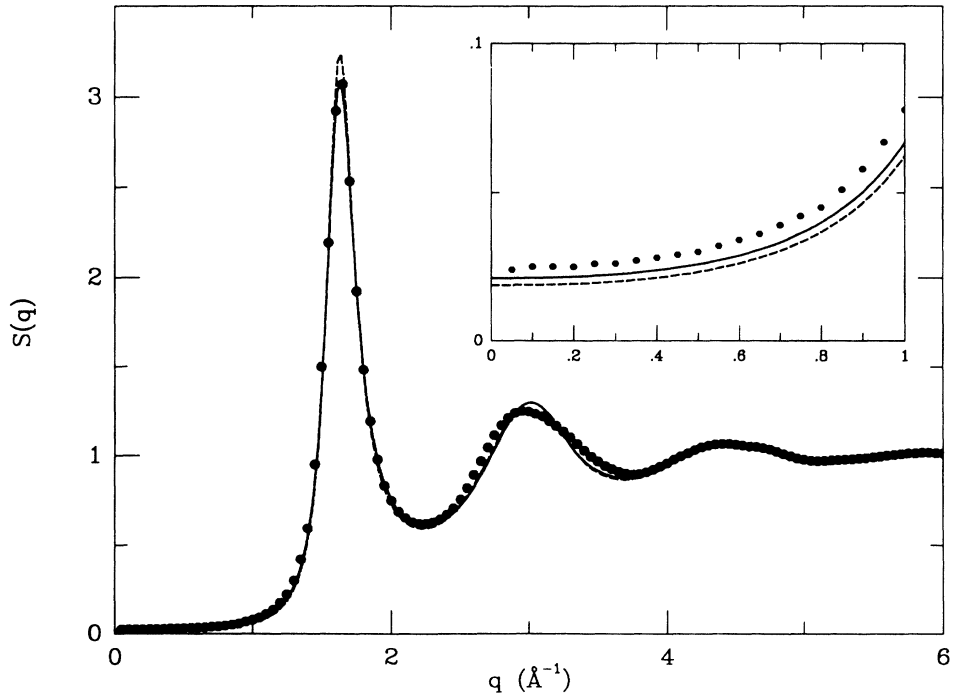

FIG. 2. Liquid-structure factor $S(q)$ for K at freezing in the MHNC-SI (full curve) and HMSA-SI (dashed curve), compared with neutron-diffraction data (solid circles) of van der Lugt and Alblas (Ref. 39). The inset in the figure shows the small-angle scattering region on an enlarged scale.

TABLE I. Temperature T, packing fraction η in the PY bridge function, mixing parameter α [in units of inverse $r_s=(3/4\pi n)^{1/3}$, n being the electronic density, see text] and the long-wavelength limit $S(0)$ calculated in the MHNC and HMSA schemes for liquid potassium at various temperatures. The second column refers to the exchange-correlation function. The experimental values $S_{\text{expt}}(0)$ are obtained either from the compressibility data quoted in Ref. 31 or from diffraction data (Ref. 66), the latter being given in parentheses.

T (°C)	Exc.-corr. function	η	α (units of r_s^{-1})	$S_{\text{MHNC}}(0)$	$S_{\text{HMSA}}(0)$	$S_{\text{expt}}(0)$
65	SI	0.4648	0.1782	0.0213	0.0189	0.0247
	IU	0.4562	0.0011	0.0260	0.0221	(0.0241)
100	SI	0.4550	0.1924	0.0231	0.0206	0.0254
	IU	0.4428	0.0009	0.0295	0.0249	
300	SI	0.3928	0.1674	0.0426	0.0373	0.0469
500	SI	0.3466	0.1567	0.0649	0.0569	0.0769
700	SI	0.3077	0.1470	0.0920	0.0811	0.1177

here and with the MHNC-IU and the HMSA-IU at $T=373$ K, we find very little (in most cases insignificant) differences from the results shown in Fig. 3.

At this point it is appropriate to make a remark in connection with a comment already made in the preceding section. We pointed out there that higher-order corrections have been taken care of in the construction of the present pair potential $V(r)$ by the GNMP theory, and emphasized that such corrections are important in the evaluation of χ_T by the LW method. Indeed, we find no difficulty in obtaining either the HMSA-SI or the HMSA-IU structure factor even at the freezing point, whereas Pastore and Kahl[30] were previously unsuccessful in applying the HMSA-IU within the context of a local pseudopotential. It thus appears that their failure to obtain a solution for α is to be attributed to the truncation at low-order perturbation theory. In addition, their values for $S(0)$ in the MHNC tend to be overestimated (see Table I in Ref. 31). This conjecture will be further supported by our MHNC-SI results for Cd presented in Sec. III C where we shall compare the MHNC-SI results for the structure factor *with* and *without*[46,63] the higher-order corrections. In summary, we emphasize that the presently adopted GNMP theory, in conjunction with the MHNC or the HMSA scheme, it quite reliable and can thus be confidently applied to the study of the liquid-structure factors of Zn and Cd.

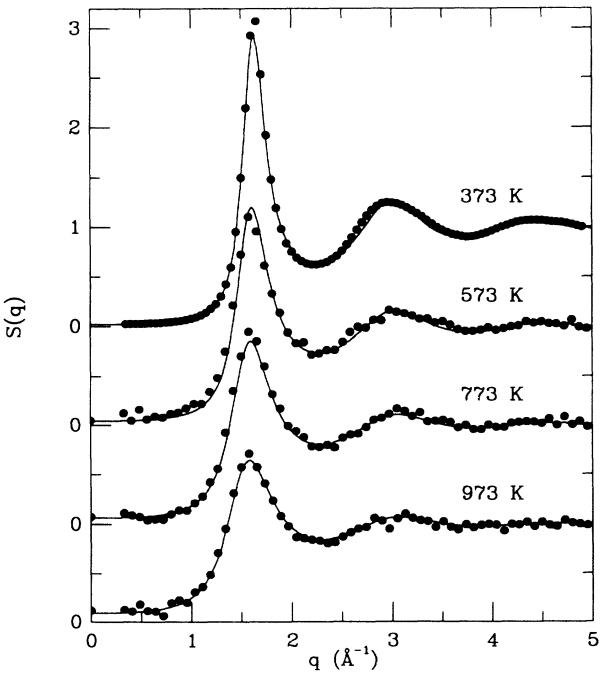

FIG. 3. Liquid-structure factor $S(q)$ for K at various temperatures, calculated using the MHNC-SI method (full curve) and compared with neutron-diffraction data (solid circles, Refs. 39 and 40).

B. Liquid zinc

Relative to simple liquid metals such as K, the liquid-structure factor of Zn is observed[41–45] to have the following features.

(a) At or near freezing at 723 K, its principal peak exhibits an asymmetric shape with respect to the position of the first maximum (q_p, say), with the low-angle side of the main maximum being appreciably less steep than the high-angle side. The subsequent oscillations of $S(q)$ are, however, not dissimilar from those of the symmetric structure factor observed in many other liquid metals.

(b) As temperature increases, the asymmetry is reduced so that at $T\simeq 923$ K the main peak in $S(q)$ has essentially regained the usual symmetric form.

The anomalous structure of divalent metals was first discussed by Weaire,[32] who extended his previous detailed study[64] of the stability of the crystalline state to a liquid analog. According to Weaire, the asymmetric behavior of the structure factor in liquid divalent metals, such as Zn and Hg, has its origin in the tendency of the liquid system to achieve a stabilized state. Specifically, he argued that these liquid metallic systems will attain a

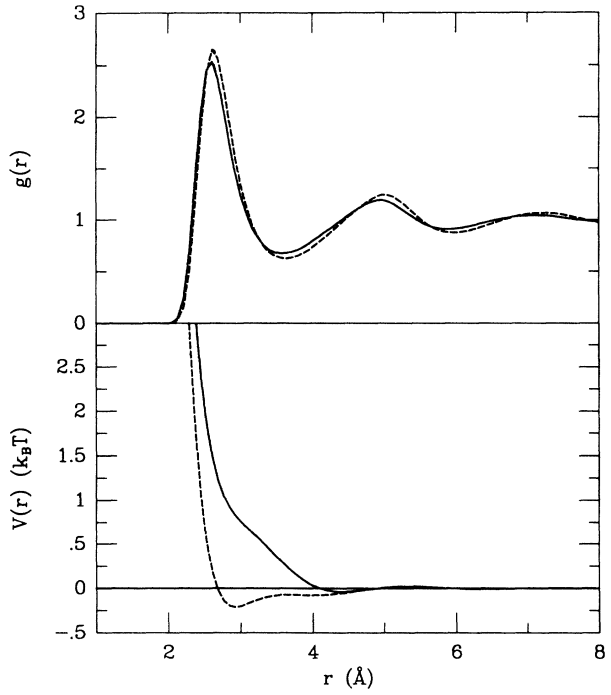

FIG. 4. The pair-correlation function $g(r)$ and interionic pair potential $V(r)$ for liquid Zn calculated at $T=723$ K in the MHNC-IU (full curve) and the MHNC-SI (dashed curve).

lower band-structure energy if their atomic structure is distorted so as to avoid the subtle crossing between the first node of the pseudopotential and the first peak position of the liquid-structure factor. To our knowledge, such an interpretation while physically appealing has not been substantiated by any realistic calculation. A more conventional "structural" calculation was put forward by Regnaut, Badiali, and Dupont[23] and by Hafner and Kahl,[24] both using the optimized RPA method to calculate $S(q)$. An interesting point that emerges from their work is that both calculations interpret such a skewed structure in Zn as due to a significant role of the long-range attractive interaction in $V(r)$. We therefore examine if the present approach can shed light on the intimate relation between the asymmetric liquid-structure factor and the long-range attractive interaction.

The bottom part of Fig. 4 shows $V(r)$ as calculated near freezing temperature for both the SI and IU exchange-correlation factors. The corresponding MHNC pair-correlation functions are displayed in the top part of Fig. 4. There are two interesting features that merit emphasis.

(a) There are clear similarities as well as differences between the SI and the IU pair potentials. In the (first) region $0 \leq r \lesssim 2.5$ Å both pair potentials show similar repulsiveness. As one proceeds into the medium-range (2.5 Å $\lesssim r \lesssim$ 4.5 Å, second region), there is a drastic

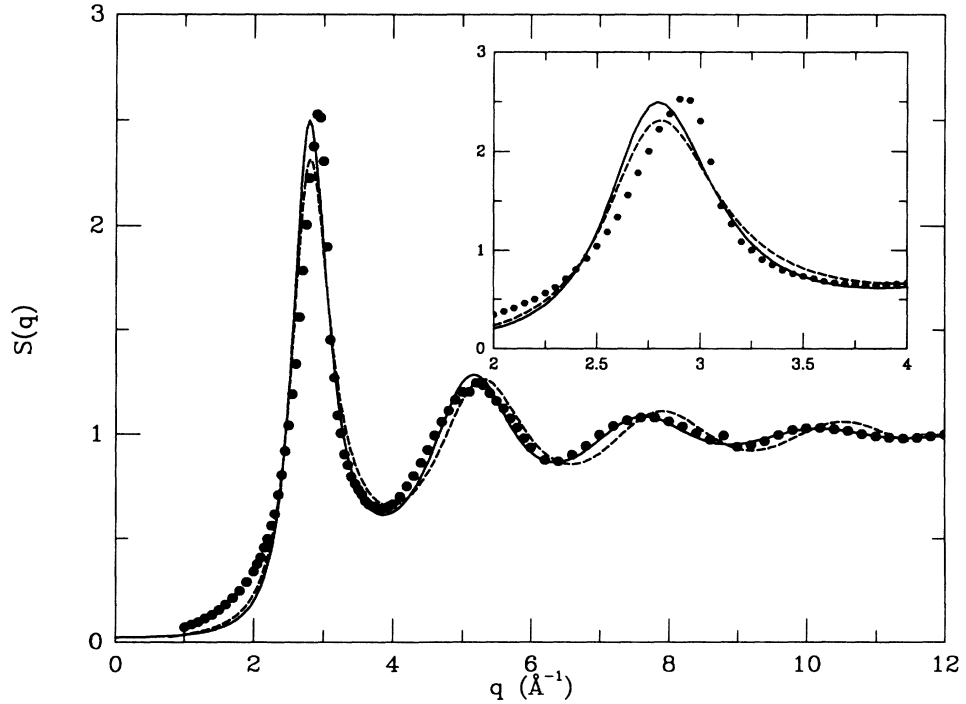

FIG. 5. Liquid-structure factor $S(q)$ for Zn calculated at $T=723$ K in the HMSA-SI approximation (full curve) compared with the charged-hard-sphere $S_{\mathrm{CHS}}(q)$ (dashed curve, Ref. 62) and with experimental data (solid circles) of Waseda (Ref. 45). The inset in the figure gives the region of the main peak on an enlarged scale.

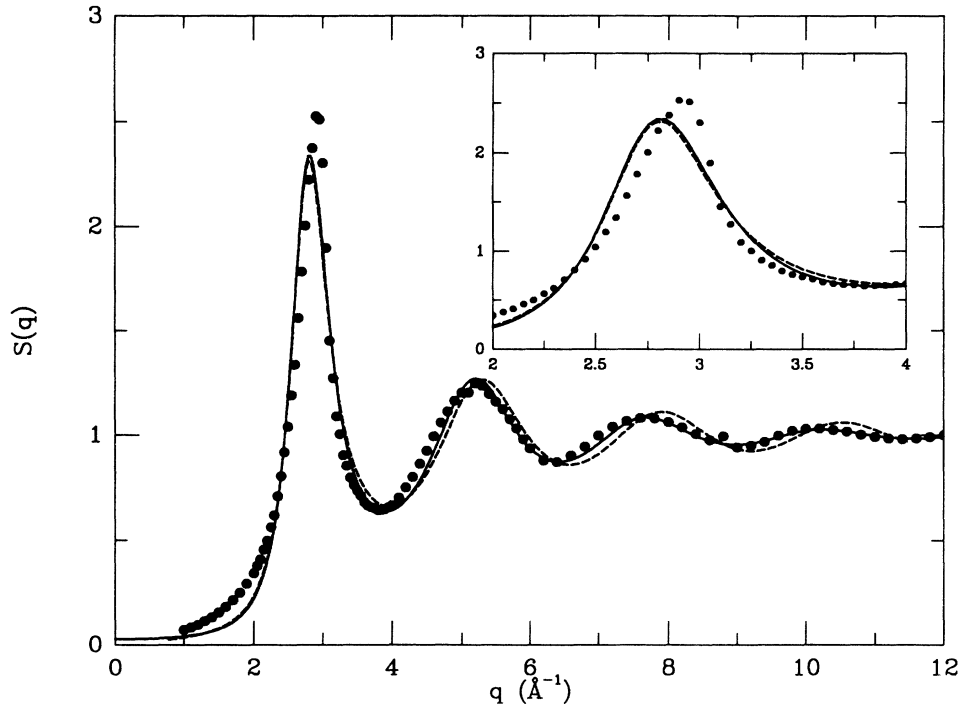

FIG. 6. Same as Fig. 5 but for MHNC-SI.

difference between the IU $V(r)$ and SI $V(r)$—the former remains repulsive but is soft and shows a faint "kink" just before the first node, whereas the latter develops its first minimum. At $r \approx 4.2$ and 4.4 Å, respectively, there is a well-defined first minimum in the IU $V(r)$ and a weak second minimum in SI $V(r)$. In the final (third) region $r \gtrsim 4.6$ Å one notices that the two potentials are essentially indistinguishable.

(b) As a result of (a) we discover that the pair-correlation functions also exhibit some subtle structure. The initial rise in slope of $g(r)$ just reflects the dominant role of the excluded-volume effect operating in the first region, which is very similar in the two potentials. However, because of the substantial differences in $V(r)$ in the second region, the MHNC-IU $g(r)$ is found to be less steep in slope on the right-hand side of the first peak

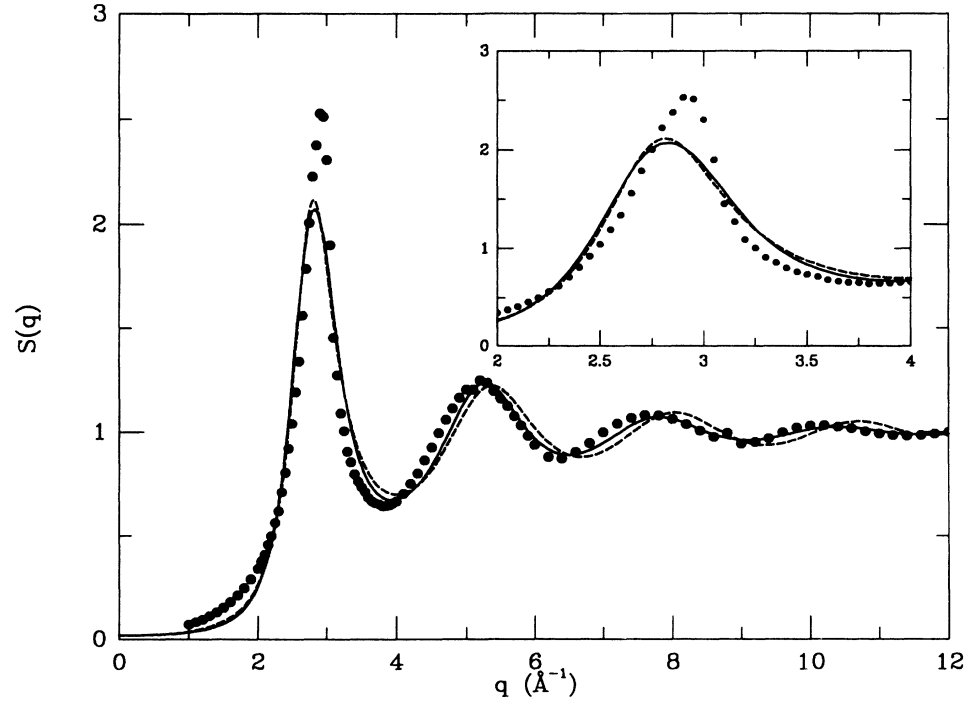

FIG. 7. Same as Fig. 5 but for HMSA-IU.

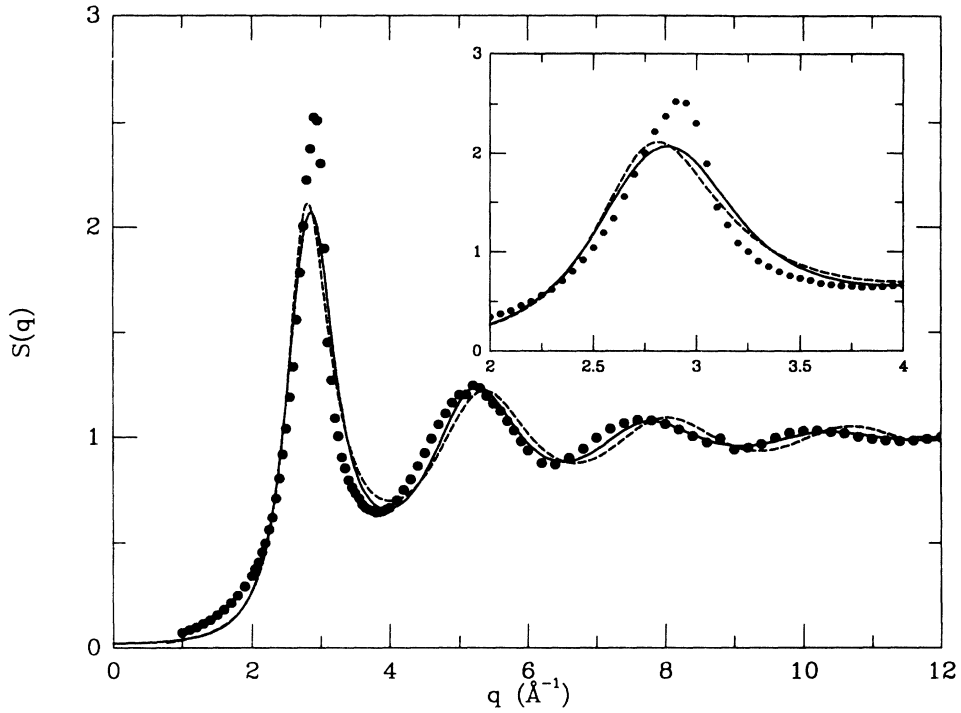

FIG. 8. Same as Fig. 5 but for MHNC-IU.

(with a tendency to "bend over" to the left). Probably because of this, the subsequent oscillations in the MHNC-IU $g(r)$ are being shifted to shorter distances relative to those in the MHNC-SI one, despite the fact that the two potentials in the third region are virtually the same.

We have repeated the above calculations in the HMSA approach. The two basic features described above remain virtually the same except for slightly enhanced oscillations of $g(r)$ in the HMSA-SI scheme. It is interesting to analyze at this point what bearing will all these features have on the liquid-structure factor $S(q)$. For this purpose we compare in Figs. 5–8 the set of four liquid-structure factors (HMSA-SI, MHNC-SI, HMSA-IU, and MHNC-IU) with (i) the charged-hard-sphere structure factor $S_{\rm CHS}(q)$,[62] which may serve as a reference for differentiating the degree of asymmetry, and (ii) the data of Waseda.[45] There are several observations that can be made.

(1) For the four calculated $S(q)$'s, the degree of reproduction of the skewed structure is in the ascending order HMSA-SI→MHNC-SI→HMSA-IU→MHNC-IU, with the MHNC-IU best explaining the asymmetric first peak. This is related to our earlier point (b) simply via Fourier transformation. Basically it is due to the IU $g(r)$ being characterized by a less steep slope on the right-hand side of its first peak. By contrast, the corresponding SI $g(r)$ has a steeper slope superimposed on an enhanced magnitude in $g(r_p)$, r_p being the position of the first maximum, which is in turn related to the first minimum of the SI $V(r)$. The general trend is clearly arising, within the nearly-free-electron pseudopotential method, from the role of exchange and correlation in dielectric screening. In addition, for a polyvalent liquid metal having a hard-type potential we would expect the MHNC to be superior

TABLE II. Temperature T, packing fraction η in the PY bridge function, mixing parameter α [in units of inverse $r_s=(3/4\pi n)^{1/3}$, n being the electronic density, see text] and the long-wavelength limit $S(0)$ calculated in the MHNC and HMSA schemes for liquid Zn at various temperatures. The second column refers to the exchange-correlation function. The value of $S_{\rm expt}(0)$ is taken from Webber and Stephens (Ref. 67).

T (°C)	Exc.-corr. function	η	α (units of r_s^{-1})	$S_{\rm MHNC}(0)$	$S_{\rm HMSA}(0)$	$S_{\rm expt}(0)$
450	SI	0.4161	0.1600	0.0284	0.0238	0.015
	IU	0.3936	0.5769	0.0216	0.0190	
560	SI	0.4005	0.1513	0.0330	0.0278	
	IU	0.3798	0.5680	0.0250	0.0221	
660	SI	0.3876	0.1466	0.0374	0.0317	
	IU	0.3681	0.5602	0.0281	0.0250	

to the HMSA, although for a given exchange-correlation function the difference between the two integral-equation schemes should not be significant.

(2) When compared with liquid potassium (Table I), we find (see Table II) that the mixing parameter α determined using the SI $V(r)$ shows regularity and is quite independent of the liquid metal under study ($\alpha \approx 0.15 r_s^{-1}$, r_s being the electron density parameter). This is not so for cases using the IU $V(r)$, where the magnitude of α for Zn is much larger than for K. Clearly, the magnitude of α reflects the shape of the potential (recall that $\alpha=0$ corresponds to the soft-core MSA). As regards the value of η, we generally obtain a lower η for Zn than for K.

(3) Except in the proximity of the main peak and in a limited region at lower wave-vector transfer, the overall agreement with experiment in all four cases is quite satisfactory, especially from near the first minimum and beyond. The discrepancy in the low-q region may be due to experimental uncertainties, since more recent experiments[41] and calculations[23] show better accord with our present results.

(4) On quantitative comparison with the observed $S(q)$, the two IU $S(q)$'s underestimate somewhat the magnitudes of the first maximum, whereas those of SI $S(q)$'s are of comparable magnitudes. We should recall, however, that there is quite a scatter of measured data, as pointed out by Wagner.[44]

As a last point we examine the temperature dependence of $S(q)$. Our MHNC-IU results for the liquid-structure factors of Zn at $T=723$, 833, and 933 K are given in Fig. 9 together with the experimental data of Waseda.[45] We notice from this figure and from the enlarged representation of the first peak in Fig. 10 that the MHNC-IU scheme predicts rather well the general behavior of $S(q)$—i.e., near freezing the first peak of $S(q)$ shows a bending towards the high-angle side and as temperature increases this asymmetric distortion gradually disappears. Over the present temperature range, howev-

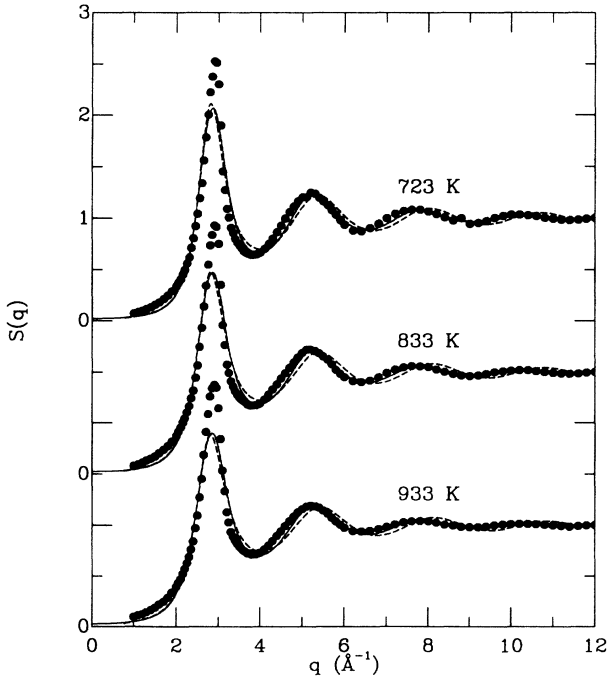

FIG. 9. Liquid-structure factor $S(q)$ for Zn calculated in the MHNC-IU (full curves), compared with charged-hard-sphere $S_{CHS}(q)$ (dashed curves, Ref. 62) and with measured data (solid circles) of Waseda (Ref. 45).

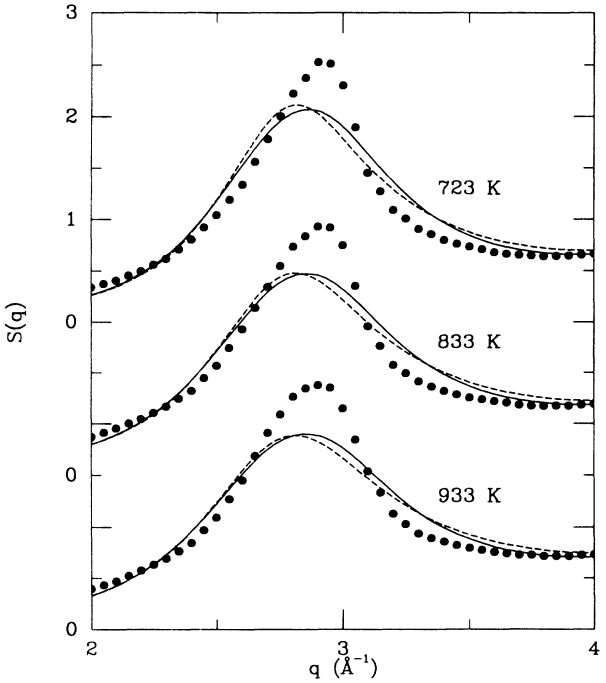

FIG. 10. Same as Fig. 9, giving an enlarged representation of the region of main peak of $S(q)$.

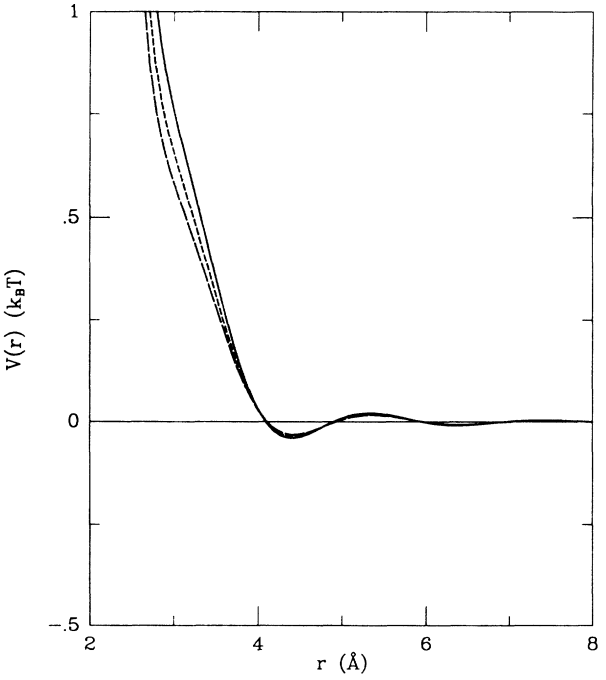

FIG. 11. The interionic pair potential IU $V(r)$ vs r for liquid Zn at $T=723$ K (full curve), 833 K (short-dashed curve), and 933 K (long-dashed curve).

TABLE III. Temperature T, position q_p (in Å^{-1}), and height $S(q_p)$ of the main peak calculated in the MHNC and HMSA approximations for liquid zinc at various temperatures. The second column refers to the exchange-correlation function.

T (°C)	Exc.-corr. function	$q_{p,\mathrm{MHNC}}$	$q_{p,\mathrm{HMSA}}$	$q_{p,\mathrm{expt}}$	$S_{\mathrm{MHNC}}(q_p)$	$S_{\mathrm{HMSA}}(q_p)$	$S_{\mathrm{expt}}(q_p)$
450	SI	2.812	2.796	2.9[a]	2.345	2.499	2.527[a]
	IU	2.860	2.826	2.89±0.02[b]	2.072	2.071	2.85±0.05[b]
560	SI	2.806	2.789	2.9[a]	2.206	2.332	2.426[a]
	IU	2.855	2.822	2.89±0.02[b]	1.975	1.976	2.67[b]
660	SI	2.801	2.783	2.9[a]	2.103	2.208	2.375[a]
	IU	2.851	2.819	2.89±0.02[b]	1.899	1.901	2.53[b]

[a]From Ref. 45.
[b]From Ref. 41, measured at temperatures of 460 °C, 550 °C, and 650 °C.

er, both the MHNC-IU and the measured $S(q)$ still continue to show some tilting, which is made evident by the comparison with $S_{\mathrm{CHS}}(q)$. Numerical results for the behavior of the main peak with temperature are given in Table III. In Fig. 11 we show the temperature variation of the IU $V(r)$. Within our earlier discussion, these changes of the pair potential (and in particular the decrease in energy of the "kink" with respect to k_BT) are clearly correlated with the behavior of $S(q)$ with increasing temperature as shown in Figs. 9 and 10.

C. Liquid cadmium

The structural behavior of liquid Cd is qualitatively similar to that of liquid Zn, but the "anomalous" behavior that we have discussed above is more marked. Specifically, the distortion of the principal peak in $S(q)$ near freezing is much more severe, and increases in temperature are less effective in restoring $S(q)$ back to the normal symmetric form, the asymmetric features being clearly present even up to the highest temperature of $T=923$ K attained in experiment.[43,44]

Applying the same integral-equation approximations to liquid Cd, the following are several of the discernible similarities and differences that we notice.

(a) The SI $V(r)$ and IU $V(r)$ pair potentials are similar in structure to those of liquid Zn (Fig. 12). The main differences are that the kink in the second region of the IU $V(r)$ is more pronounced and the second minimum of the SI $V(r)$ is well developed. As a consequence, we find that the "bend-over" of the IU $g(r)$ towards the left-hand side of its first maximum [relative to the SI $g(r)$] is slightly more pronounced than in Zn (Fig. 12).[65] Such a distor-

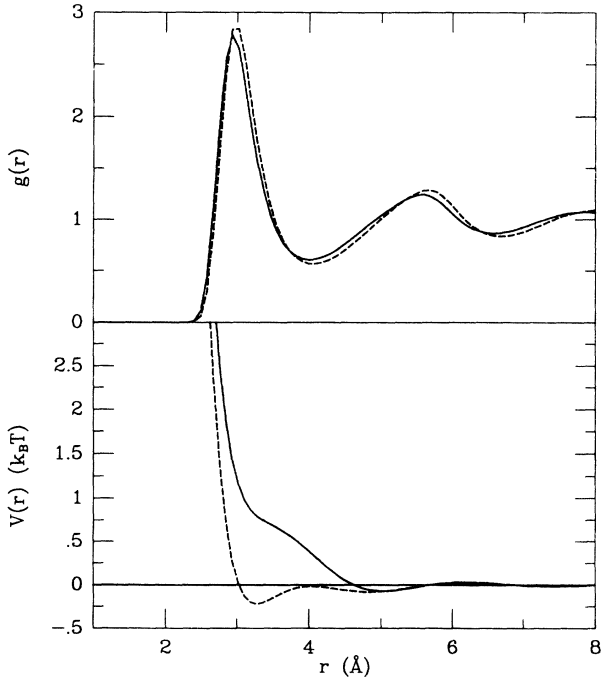

FIG. 12. The pair-correlation function $g(r)$ and interionic pair potential $V(r)$ for liquid Cd calculated at $T=623$ K in the MHNC-IU (full curve) and the MHNC-SI (dashed curve).

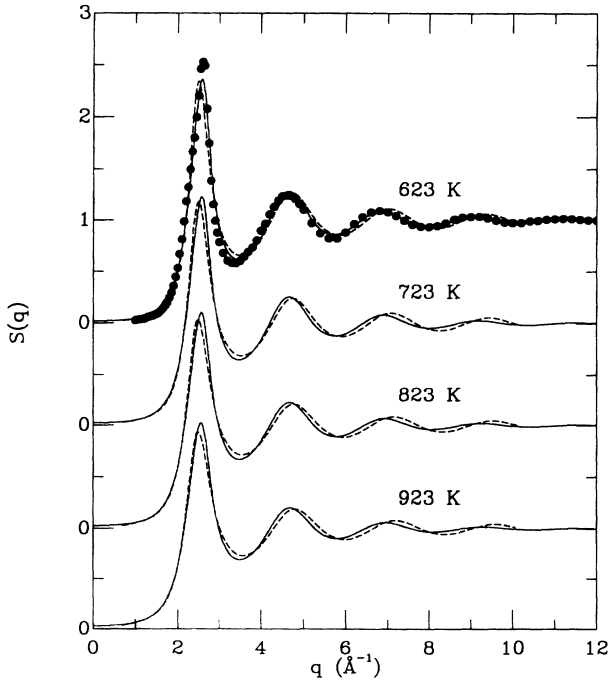

FIG. 13. Liquid-structure factor $S(q)$ for Cd in the MHNC-IU (full curves), compared with $S_{\mathrm{CHS}}(q)$ (dashed curves, Ref. 62) and with measured data (solid circles) at $T=623$ K of Waseda (Ref. 45).

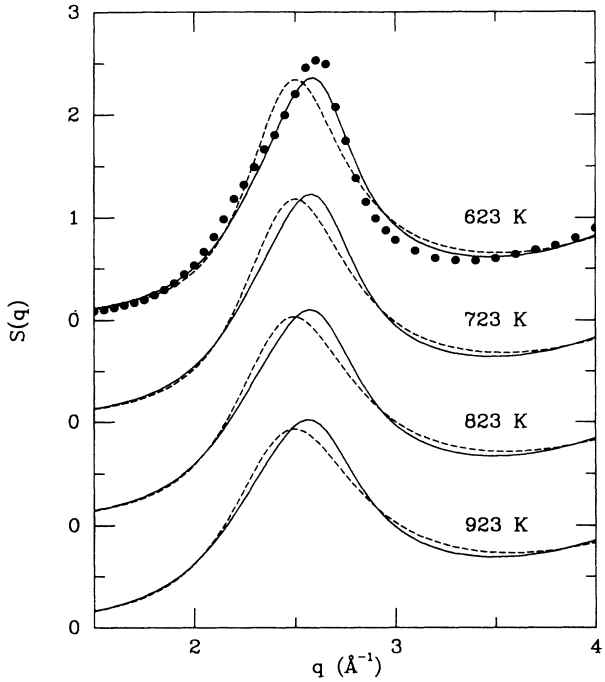

FIG. 14. Same as Fig. 13, giving an enlarged representation of the region of the main peak of $S(q)$.

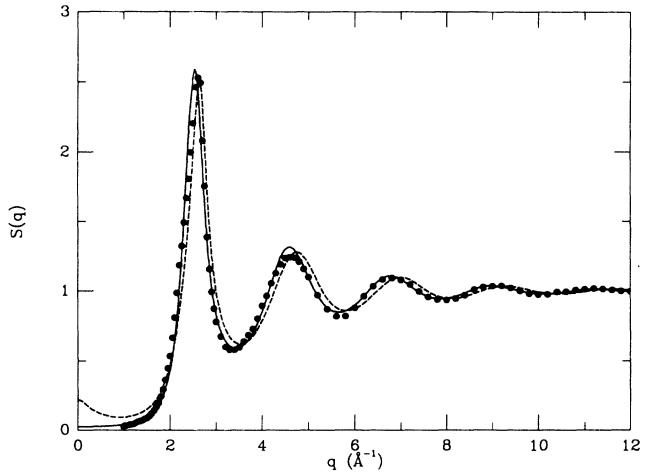

FIG. 15. Liquid-structure factor $S(q)$ for Cd near freezing calculated in the MHNC-SI with an energy-independent nonlocal model pseudopotential (dashed curve) and with the GNMP (full curve).

tion accounts for the more asymmetric shape of the main peak in $S(q)$, as borne out in our MHNC-IU results and further corroborated by their very good agreement with experiment (Figs. 13 and 14).

(b) In accordance with our earlier discussion for Zn we find that our α values for HMSA-SI near freezing and at higher temperatures are also about $0.15 r_s^{-1}$, whereas those for HMSA-IU remain noticeably dependent on the shape of $V(r)$. The η values in the MHNC scheme are again somewhat small compared with those appropriate to liquid K. All these results are collected in Table IV.

(c) The temperature dependence of $S(q)$ for the MHNC-IU case is shown in Figs. 13 and 14. The agreement with experiment is much better than for Zn, for what concerns particularly the skewed shape of the main peak. The temperature variation of q_p and $S(q_p)$ for Cd is reported in Table V.

Finally, we should comment on a relevant work by Hafner and Kahl.[24] These authors attempted to explain the trend of the liquid-structure factor for many simple liquid metals using the optimized WCA RPA in conjunction with a local empty-core pseudopotential. For liquid Cd, they showed that an atypical pair potential similar in form to the IU $V(r)$ in Fig. 12 is a prerequisite for producing an asymmetric $S(q)$. While this observation is generally in line with our earlier discussion, one should also note that the underlying physics for the liquid-structure factor turns out to be more subtle. This can be seen from our MHNC-SI $S(q)$ given in Fig. 15, where we compare the results obtained from the energy-independent nonlocal model pseudopotential, for which the higher-order corrections are omitted,[46,63] and from the GNMP theory. It is evident that even the theory

TABLE IV. Temperature T, packing fraction η in the PY bridge function, mixing parameter α [in units of inverse $r_s=(3/4\pi n)^{1/3}$, n being the electronic density, see text] and the long-wavelength limit $S(0)$ calculated in the MHNC and HMSA schemes for liquid Cd at various temperatures. The second column refers to the exchange-correlation function. The value of $S_{\text{expt}}(0)$ is taken from Webber and Stephens (Ref. 67).

T (°C)	Exc.-corr. function	η	α (units of r_s^{-1})	$S_{\text{MHNC}}(0)$	$S_{\text{HMSA}}(0)$	$S_{\text{expt}}(0)$
350	SI	0.4314	0.1588	0.0246	0.0202	0.011
	IU	0.4049	0.5100	0.0208	0.0177	
450	SI	0.4166	0.1537	0.0284	0.0235	
	IU	0.3914	0.5001	0.0239	0.0206	
550	SI	0.4022	0.1468	0.0327	0.0272	
	IU	0.3783	0.5005	0.0271	0.0236	
650	SI	0.3890	0.1408	0.0372	0.0311	
	IU	0.3662	0.4800	0.0309	0.0270	

TABLE V. Temperature T, position q_p (in Å^{-1}), and height $S(q_p)$ of the main peak calculated in the MHNC and HMSA approximations for liquid Cd at various temperatures. The second column refers to the exchange-correlation function.

T (°C)	Exc.-corr. function	$q_{p,\mathrm{MHNC}}$	$q_{p,\mathrm{HMSA}}$	$q_{p,\mathrm{expt}}$	$S_{\mathrm{MHNC}}(q_p)$	$S_{\mathrm{HMSA}}(q_p)$	$S_{\mathrm{expt}}(q_p)$
350	SI	2.531	2.515	2.62[a]	2.590	2.771	2.54[a]
	IU	2.583	2.562	2.57[b]	2.365	2.334	2.55[b]
450	SI	2.525	2.518	2.56[b]	2.432	2.578	2.45[b]
	IU	2.577	2.556		2.234	2.213	
550	SI	2.518	2.500	2.55[b]	2.296	2.415	2.38[b]
	IU	2.571	2.550		2.104	2.088	
650	SI	2.511	2.493	2.54[b]	2.182	2.281	2.24[b]
	IU	2.563	2.543		2.026	2.014	

[a]From Ref. 45.
[b]From Refs. 43 and 44.

without higher-order corrections may yield fortuitously an asymmetric structure for the main peak but it badly fails, as in the work of Hafner and Kahl,[24] in the lower and higher momentum-transfer regions.

IV. SUMMARY AND CONCLUDING REMARKS

In this work, using a highly reliable GNMP theory and two different exchange-correlation functions, we have constructed interionic pair potentials for the liquid metals Zn and Cd at freezing and at a few temperatures above freezing, as well as an interionic pair potential for liquid K. As a means to ascertain the accuracy of the present approach, and also with a view to interpreting the recent neutron-diffraction data for this latter element, we have carried out calculations of its liquid structure within the MHNC and the HMSA integral-equation schemes. We have obtained remarkably good agreement with computer simulation data and with experiments.

We have then proceeded to apply the same techniques to an investigation of the liquid structure of Zn and Cd. We have analyzed the intimate connection between the interionic pair potential $V(r)$ and the pair-correlation function and found that the medium-range and long-range attractive parts of $V(r)$ are indeed crucial for a quantitative understanding of the asymmetric distortion of the main peak in $S(q)$ in these divalent liquid metals. This conclusion is in accord with the earlier calculation on liquid Zn by Regnaut, Badiali, and Dupont[23] who used the optimized WCA RPA for a similar purpose. As far as our calculations show, the exchange-correlation factor of Ichimaru and Utsumi is quite accurate, beside being computationally simple, and can thus be quite confidently used for quantitative studies of $S(q)$ and possibly for thermodynamic and electronic properties. A similar conclusion has been reached by Kahl and Hafner[12] in their investigation of expanded liquid Rb. We have also stressed the role of higher-order perturbative corrections in the construction of the bare-ion pseudopotential. However, both nonlinear corrections and the nature of exchange and correlation in the electron gas do not easily lead to a deeper understanding of systems such as Zn and Cd in terms of electronic structure or chemical bonding.

Underlying the success of the present integral-equation approximations is the method of long waves to the isothermal compressibility χ_T, which we have taken together with $S(0)$ to determine the parameters η and α subject to the condition of statistical-mechanical self-consistency. Bearing in mind that our pseudopotential is treated beyond second-order perturbation theory, our theoretical results for $g(r)$ and $S(q)$ are built on firm grounds. It would be interesting, however, to examine also the homogeneous deformation route for imposing thermodynamic self-consistency.

ACKNOWLEDGMENTS

We are very grateful to Dr. G. Pastore for providing us with his MHNC and HMSA computer programs and to Dr. J. F. Jal for making available his experimental results on liquid K prior to publication. This work has been supported in part by the National Sciences Council, Taiwan, Republic of China under Contract No. NSC79-0208-M008-23 and by the Ministero della Universita' e della Ricerca Scientifica e Tecnologica of Italy. Two of us (S.K.L. and W.L.) wish to thank Professor Abdus Salam, the International Atomic Energy Agency, and UNESCO for hospitality at the International Centre for Theoretical Physics in Trieste.

[1]D. Fincham and D. M Heyes, in *Advances in Chemical Physics,* edited by M. W. Evans (Wiley-Interscience, New York, 1985), Vol. 63, p. 493.
[2]W. W. Wood, in *Physics of Simple Fluids,* edited by H. N. V. Temperley, G. S. Rushbrooke, and J. S. Rowlinson (North-Holland, Amsterdam, 1968), Chap. 5.
[3]Y. Rosenfeld and N. W. Ashcroft, Phys. Rev. A **20**, 1208 (1979).
[4]J. A. Barker and D. Henderson, Rev. Mod. Phys. **48**, 587 (1976).

[5]J. P. Hansen and I. R. MacDonald, *The Theory of Simple Liquids* (Academic, London, 1986).
[6]N. W. Ashcroft and D. Stroud, in *Solid State Physics,* edited by F. Seitz, D. Turnbull, and H. Ehrenreich (Academic, New York, 1978), Vol. 33, p. 1.
[7]W. H. Young, in *Liquid Metals, 1976,* IOP Conference Proceeding, edited by R. Evans and D. A. Greenwood (Institute of Physics and Physical Society, London, 1977), Vol. 30, p. 1.
[8]J. D. Weeks, D. Chandler, and H. C. Andersen, J. Chem. Phys. **54**, 5237 (1971).
[9]R. Kumaravadivel and R. Evans, J. Phys. C **9**, 3877 (1976).
[10]R. E. Jacobs and H. C. Andersen, Chem. Phys. **10**, 73 (1975).
[11]M. E. Telo da Gama and R. Evans, Mol. Phys. **41**, 1091 (1980).
[12]G. Kahl and J. Hafner, Phys. Rev. A **29**, 3310 (1984).
[13]J. L. Bretonnet and C. Regnaut, Phys. Rev. B **31**, 5071 (1985).
[14]G. Kahl and J. Hafner, Z. Phys. B **58**, 283 (1985).
[15]C. Regnaut, J. Phys. F **16**, 296 (1986).
[16]R. Evans and W. Schirmacher, J. Phys. C **11**, 2437 (1978).
[17]R. Evans and T. J. Sluckin, J. Phys. C **14**, 2659 (1981).
[18]R. Evans and T. J. Sluckin, J. Phys. C **14**, 3137 (1981).
[19]D. K. Chaturvedi, G. Senatore, and M. P. Tosi, Lett. Nuovo Cimento **30**, 47 (1981).
[20]D. K. Chaturvedi, M. Rovere, G. Senatore, and M. P. Tosi, Physica B **111**, 11 (1981).
[21]In addition to the WCA and OCP-RPA methods, Singh and Holz [Phys. Rev. A **28**, 1108 (1983); **29**, 1554 (1984)] have proposed a charged-hard-sphere RPA for liquid-alkali metals. Their approach is equivalent to setting $S_{\rm ref}(q) \equiv S_{\rm CHS}(q;\sigma,\Gamma)$, Γ being the usual plasma parameter.
[22]H. C. Andersen, D. Chandler, and J. D. Weeks, J. Chem. Phys. **56**, 3812 (1972); Adv. Chem. Phys. **35**, 105 (1976).
[23]C. Regnaut, J. P. Badiali, and M. Dupont, Phys. Lett. A **74**, 245 (1979); J. Phys. (Paris) Colloq. **41**, C8-603 (1980).
[24]J. Hafner and G. Kahl, J. Phys. F **14**, 2259 (1984).
[25]G. Pastore and M. P. Tosi, Physica B **124**, 383 (1984).
[26]In a subsequent work Kahl and Hafner (Ref. 14) reported optimized WCA-RPA results for liquid Rb at $T=319$ K, but without full technical details. In a very recent calculation using the Gibbs-Bogoliubov variational theory [S. K. Lai, O. Akinlade, and M. P. Tosi, Phys. Rev. A **41**, 5482 (1990)], we demonstrated the superiority of the charged-hard-sphere fluid over the neutral-hard-sphere fluid as a reference system and showed that the liquid-structure factor is quite insensitive to changes in the plasma parameter Γ, provided that a reasonable means is used to determine σ. With the Gillan criterion [M. J. Gillan, J. Phys. C **7**, L1 (1974)] for fixing σ, the only *tunable* parameter in the optimized OCP RPA is Γ, which Pastore and Tosi set to the true valence. We thus believe that the reference $S(q)$ will not be much affected by determining Γ through a self-consistency condition. From this point of view, the iterative self-consistency condition in the standard optimized RPA is inconsequential in the optimized OCP RPA, at least for alkali metals. Our argument is supported by the close similarity between the *true* and the predicted *optimal* potentials for wave numbers below the position of the main peak in the structure factor (see Fig. 3 in Ref. 25).
[27]M. J. Gillan, Mol. Phys. **38**, 1781 (1979); G. Zerah, J. Comput. Phys. **61**, 280 (1985).
[28]F. Lado, Phys. Lett. **89**, 196 (1982); F. Lado, S. M. Foiles, and N. W. Ashcroft, Phys. Rev. A **28**, 2374 (1983).
[29]G. Zerah and J. P. Hansen, J. Chem. Phys. **84**, 2336 (1986).
[30]G. Pastore and G. Kahl, J. Phys. F **17**, L267 (1987).
[31]G. Kahl and G. Pastore, Europhys. Lett. **7**, 37 (1988).
[32]D. Weaire, J. Phys. C **1**, 210 (1968).
[33]D. H. Li, X. R. Li, and S. Wang, J. Phys. F **16**, 309 (1986).
[34]F. J. Rogers, D. A. Young, H. E. DeWitt, and M. Ross, Phys. Rev. A **28**, 2990 (1983).
[35]M. Hasegawa and M. Watabe, J. Phys. C **18**, 2081 (1985).
[36]K. Hoshino, M. Matsuda, H. Mori, and M. Watabe, J. Non-Cryst. Solids **117/118**, 44 (1990).
[37]Aside from this reason, another motive for examining method (ii) has been inspired by the comparative studies of high-pressures fluids by J. Talbot, J. L. Lebowitz, E. M. Waisman, D. Levesque, and J. J. Weis [J. Chem. Phys. **85**, 2187 (1987)] who demonstrated the superiority of the HMSA integral equation over other perturbative theories.
[38]A technically similar hybridized integral equation, from which the HMSA evolves, has in fact been proposed previously. This so-called Rogers-Young integral equation [F. J. Rogers and D. A. Young, Phys. Rev. A **30**, 999 (1984)] has so far been tested successfully only for simple liquids such as inverse potential fluids and the one-component plasma. Recently the Rogers-Young integral-equation method has been applied also to a supercooled soft-sphere plus Kac potential liquid [S. Kambayashi and Y. Hiwatari, Phys. Rev. A **37**, 852 (1988)], but the predicted supercooled liquid structure is merely of moderate quality.
[39]W. van der Lugt and B. P. Alblas, in *Handbook of Thermodynamic and Transport Properties of Alkali Metals,* edited by R. W. Ohse (Blackwell, Oxford, 1985).
[40]J. F. Jal, C. Mathieu, and J. Dupuy (unpublished).
[41]W. Knoll, in *Liquid Metals, 1976,* IOP Conference Proceeding, edited by R. Evans and D. A. Greenwood (Institute of Physics and Physical Society, London, 1977), Vol. 30, p. 117.
[42]D. F. Wingfield and J. E. Enderby, Phys. Lett. A **27**, 704 (1968).
[43]D. M. North and C. N. J. Wagner, Phys. Lett. A **30**, 440 (1969).
[44]C. N. J. Wagner, in *Liquid Metals, 1976,* IOP Conference Proceeding, edited by R. Evans and D. A. Greenwood (Institute of Physics and Physical Society, London, 1977), Vol. 30, p. 110.
[45]Y. Waseda, *The Structure of Non-Crystalline Materials* (McGraw-Hill, New York, 1980).
[46]S. Wang and S. K. Lai, J. Phys. F **10**, 2717 (1980).
[47]In addition to thermodynamic properties [Ref. 34; S. K. Lai, Phys. Rev. A **38**, 5707 (1988); S. K. Lai, O. Akinlade, and M. P. Tosi, Phys. Rev. A **41**, 5482 (1990)], the reliability of the GNMP has been demonstrated in a number of computer simulation studies of liquid and amorphous metals [S. K. Lai, S. Wang, and K. P. Wang, J. Chem. Phys. **87**, 559 (1987); S. K. Lai, J. Phys. F **18**, 1663 (1988); **18**, 1673 (1988); H. Nakano, D. W. Qi, and S. Wang, J. Chem. Phys. **90**, 1871 (1989)] as well as in the calculation of surface properties [S. K. Lai, J. Chem. Phys. **86**, 2095 (1987); S. K. Lai, and S. Wang, Z. Phys. Chem. **156**, 451 (1988)] and of magnetic susceptibility [S. K. Lai, High Temp. Mater. Processes **8**, 241 (1989)].
[48]S. M. Folies, N. W. Ashcroft, and L. Reatto, J. Chem. Phys. **80**, 4441 (1984); P. D. Poll and N. W. Ashcroft, Phys. Rev. A **32**, 1722 (1985); **35**, 866 (1987). The latter two references are devoted to the critical behavior of fluids.
[49]H. Iyetomi and S. Ichimaru, Phys. Rev. A **27**, 3241 (1983); P. Ballone, G. Pastore, and M. P. Tosi, J. Chem. Phys. **81**, 3174 (1984); S. Kambayashi and Y. Hiwatari, Phys. Rev. A **41**, 1990 (1990).

[50]M. S. Wertheim, Phys. Rev. Lett. **10**, 321 (1963).
[51]E. Thiele, J. Chem. Phys. **30**, 474 (1963).
[52]W. G. Madden and S. A. Rice, J. Chem. Phys. **72**, 4208 (1980).
[53]D. L. Price, Phys. Rev. A **4**, 358 (1971).
[54]M. Hasegawa and M. Watabe, J. Phys. Soc. Jpn. **32**, 14 (1972).
[55]M. Hasegawa and W. H. Young, J. Phys. F **11**, 977 (1981).
[56]N. W. Ashcroft and D. C. Langreth, Phys. Rev. **155**, 682 (1967).
[57]I. H. Umar, A. Meyer, M. Watabe, and W. H. Young, J. Phys. F **4**, 1691 (1974).
[58]H. D. Jones, J. Phys. C **6**, 2833 (1973).
[59]R. Kumaravadivel, J. Phys. F **13**, 1607 (1983).
[60]K. S. Singwi, A. Sjolander, M. P. Tosi, and R. H. Land, Phys. Rev. B **1**, 1044 (1970).
[61]S. Ichimaru and K. Utsumi, Phys. Rev. B **24**, 7385 (1981).
[62]O. Akinlade, S. K. Lai, and M. P. Tosi, Physica B **167**, 61 (1990).
[63]C. H. Woo, S. Wang, and M. Matsuura, J. Phys. F **5**, 1836 (1975).
[64]V. Heine and D. Weaire, Phys. Rev. **152**, 603 (1966).
[65]Below we shall in most cases present the MHNC-IU results for the reason that they generally are slightly more compatible with the available measured data. The quality of other results is either similar to that discussed for liquid Zn or basically the same as the MHNC-IU.
[66]M. J. Huijben and W. van der Lugt, Acta Crystallogr. A **35**, 431 (1979).
[67]G. M. B. Webber and R. W. B. Stephens, in *Physical Acoustics,* edited by W. P. Mason (Academic, New York, 1968), Vol. 4B, p. 53.